Decline in arylsulfatase B expression increases EGFR expression by inhibiting the protein-tyrosine phosphatase SHP2 and activating JNK in prostate cells

Received for publication, December 2, 2017, and in revised form, May 14, 2018 Published, Papers in Press, May 24, 2018, DOI 10.1074/jbc.RA117.001244

Sumit Bhattacharyya[‡], Leo Feferman[‡], Xiaorui Han[§], Yilan Ouyang[§], Fuming Zhang[§], Robert J. Linhardt[§], and Joanne K. Tobacman[‡1]

From the [‡]Department of Medicine, University of Illinois and Jesse Brown Veterans Affairs Medical Center, Chicago, Illinois 60612 and the [§]Departments of Chemistry and Chemical Biology, Chemical and Biological Engineering, and Biology and Biomedical Engineering and the Center for Biotechnology and Interdisciplinary Studies, Rensselaer Polytechnic Institute, Troy, New York 12180

Edited by John M. Denu

Epidermal growth factor receptor (EGFR) has a crucial role in cell differentiation and proliferation and cancer, and its expression appears to be up-regulated when arylsulfatase B (ARSB or GalNAc-4-sulfatase) is reduced. ARSB removes 4-sulfate groups from the nonreducing end of dermatan sulfate and chondroitin 4-sulfate (C4S), and its decreased expression has previously been reported to inhibit the activity of the ubiquitous protein-tyrosine phosphatase, nonreceptor type 11 (SHP2 or PTPN11). However, the mechanism by which decline in ARSB leads to decline in SHP2 activity is unclear. Here, we show that SHP2 binds preferentially C4S, rather than chondroitin 6-sulfate, and confirm that SHP2 activity declines when ARSB is silenced. The reduction in ARSB activity, and the resultant increase in C4S, increased the expression of EGFR (Her1/ErbB1) in human prostate stem and epithelial cells. The increased expression of EGFR occurred after 1) the decline in SHP2 activity, 2) enhanced c-Jun N-terminal kinase (JNK) activity, 3) increased nuclear DNA binding by c-Jun and c-Fos, and 4) EGFR promoter activation. In response to exogenous EGF, there was increased bromodeoxyuridine incorporation, consistent with enhanced cell proliferation. These findings indicated that ARSB and chondroitin 4-sulfation affect the activation of an important dual phosphorylation threonine–tyrosine kinase and the mRNA expression of a critical tyrosine kinase receptor in prostate cells. Restoration of ARSB activity with the associated reduction in C4S may provide a new therapeutic approach for managing malignancies in which EGFR-mediated tyrosine kinase signaling pathways are active.

The epidermal growth factor receptor (EGFR)[2] has a crucial role in cell differentiation and proliferation. When first identified, it was considered to be the primary determinant of epithelial development, and the EGFR has been targeted by multiple antibodies in the search for effective cancer treatment (1–5). The Erb family of receptors, including ERBB1 (EGFR), ERBB2 (Her2/Neu), ERBB3, and ERBB4, comprise a family of cell surface receptors that are identified as critical mediators of cellular signaling (6, 7). EGFR is a tyrosine kinase receptor, with an extracellular domain, a transmembrane domain, and a cytoplasmic domain that coordinate to respond to exogenous ligands. The predominant ligand is epidermal growth factor (EGF), but other cytokines, such as transforming growth factor (TGF)-α, can also bind to the extracellular domain (8, 9). Binding of ligand to EGFR induces a conformational change in the receptor and facilitates homo- and heterodimerization of the receptor, leading to activation of tyrosine kinase activity. The phosphorylation of tyrosine residues in the cytoplasmic domain of the receptor activates intracellular signaling (10). Her2/Neu does not require ligand binding for activation and is available for dimerization with other ERB family receptors (6). Chemotherapeutic regimens have been developed with antibodies targeted to the EGFR extracellular domain, as well as to Her2/Neu and ERBB3 (1–7). Targeting of EGFR and Erb family receptors has not yet been shown to be effective treatment for prostate cancer, possibly due to the complex interaction between the EGFR and the androgen receptor or activation of alternative signaling pathways (11–14).

This report presents the pathway by which decline in activity of the enzyme arylsulfatase B (ARSB; GalNAc-4-sulfatase) increases the mRNA expression of EGFR. Previously, we reported that ARSB was reduced in malignant prostate tissue, compared with normal prostate tissue, and that lower ARSB immunohistochemical scores were associated with higher Gleason scores and biochemical recurrences in prostate cancers (15, 16). Also, in the prostate malignancies or when ARSB was silenced in normal prostate epithelial and stromal cells,

This work was supported by the University of Illinois Cancer Center. The authors declare that they have no conflicts of interest with the contents of this article.

[1] To whom correspondence should be addressed: Dept. of Medicine, University of Illinois, 840 S. Wood St. CSN 440, M/C 718, Chicago, IL 60612. Tel.: 312-569-7826; Fax: 312-413-8283; E-mail: jkt@uic.edu.

[2] The abbreviations used are: EGFR, epidermal growth factor receptor; EGF, epidermal growth factor; NaBH3CN, sodium cyanoborohydride; AP-1, activating protein 1; ARSB, arylsulfatase B or GalNAc-4-sulfatase; CA, constitutively active; cJMP, c-Jun mimetic peptide; DN, dominant negative; PHPS1, phenylhydrazonopyrazolone sulfonate; SHP2, tyrosine-protein phosphatase nonreceptor type 11 or PTPN11; TGF, transforming growth factor; C4S and C6S, chondroitin 4-sulfate and chondroitin 6-sulfate, respectively; GAG, glycosaminoglycan; JNK, c-Jun N-terminal kinase; JIP-1, JNK-selective inhibitor peptide; BrdU, 5-bromo-2′-deoxyuridine; ERK, extracellular signal-regulated kinase; AMAC, 2-aminoacridone; MPA, mobile phase A; GST, glutathione *S*-transferase; RT, room temperature; HRP, horseradish peroxidase.

there was increased expression of the extracellular matrix proteoglycan versican and of EGFR (15, 17). The increased expression of versican was due to transcriptional effects of galectin-3 and AP-1 on the versican promoter (17). Galectin-3 bound less to the more highly sulfated chondroitin 4-sulfate (C4S), which was present when ARSB activity was reduced. Galectin-3 was more abundant in cell nuclei, where it contributed to AP-1–mediated transcriptional effects on versican. Other transcriptional events were also affected by the decline in binding of galectin-3 with C4S when ARSB was reduced (17–20). However, galectin-3 silencing did not inhibit the expression of EGFR in the prostate cells (as shown in this report). In other experiments in hepatic cells, melanocytes, and prostate stem cells, transcriptional effects due to the decline of ARSB and the concomitant increase in C4S were attributed to the inhibition of activity of the ubiquitous nonreceptor tyrosine phosphatase SHP2 (protein-tyrosine phosphatase 11 (PTPN11)) (19, 21, 22). This report presents the mechanism by which SHP2 inhibition following decline in ARSB and increase in C4S can regulate EGFR expression in prostate cells and tissue.

Results

Decline in ARSB and associated increase in total sulfated glycosaminoglycans and chondroitin 4-sulfate in human prostate epithelial cells and stem cells

Arylsulfatase B activity was determined in human prostate epithelial cells and stem cells following ARSB silencing by siRNA and overexpression by ARSB plasmid using the exogenous substrate 4-methylumbelliferyl sulfate (17, 22). Effectiveness of the knockdown and overexpression was demonstrated (Table 1). There were no significant differences in activity between the epithelial and stem cells, although activity was greater in the epithelial cells. When ARSB activity was measured in malignant and normal human prostate tissue, activity was significantly greater in the normal tissue (139 ± 13 nmol/mg of protein/h *versus* 76 ± 7 nmol/mg of protein/h; n = 9) (15).

Consistent with the decline in ARSB following ARSB knockdown by siRNA, the total sulfated glycosaminoglycans (GAGs), including C4S, chondroitin 6-sulfate (C6S), dermatan sulfate, keratan sulfate, heparin, and heparan sulfate, were markedly increased in the prostate stem and epithelial cells when measured by the Blyscan assay, as reported previously (17, 22). The increases were largely attributable to the increase in C4S, and the C6S was unchanged by the changes in ARSB (Table 2). C4S and C6S were quantified by the Blyscan assay following immunoprecipitation with specific antibodies, as reported previously (17, 22).

Table 1
ARSB activity in human prostate epithelial and stem cells
Results shown are the mean ± S.D. See Refs. 17 and 22.

	Epithelial cells	Stem cells
	nmol/mg protein/h	
Control	110.6 ± 6.8	88.4 ± 4.8
Control siRNA	116.0 ± 5.6	88.1 ± 3.1
ARSB siRNA	8.8 ± 0.8	7.8 ± 0.1
Silencing efficiency (%)	92%	89%
Vector control	106.9 ± 5.6	87.4 ± 8.3
ARSB overexpression	260.2 ± 13.7	199.4 ± 18.7
Overexpression (%)	243%	228%

EGFR is increased in prostate stem cells following ARSB silencing and SHP2 inhibition

EGFR had previously been shown to be increased in the prostate epithelial cells when ARSB was silenced (17) and in the malignant prostate tissue (15), but the mechanism was unknown. Consistent with these previous findings, in the prostate stem cells, ARSB silencing increased and ARSB overexpression reduced the expression of EGFR (Fig. 1*A*). Western blotting confirms the increase in EGFR protein when ARSB was silenced by siRNA (Fig. 1*B*). Treatment with galectin-3 siRNA or with the Sp1 inhibitor (mithramycin) did not block the increase in EGFR expression that followed ARSB silencing. In contrast, the AP-1 DNA binding inhibitor SR11302 significantly reduced the EGFR expression in the stem cells (Fig. 1*C*). The SHP2 inhibitor PHPS1 and the c-Jun mimetic peptide (cJMP) also significantly reduced the expression of EGFR in the prostate stem and epithelial cells (Fig. 1*D*), suggesting that effects on SHP2 and JNK may mediate the effects of ARSB silencing on EGFR expression.

The SHP2 activity was previously reported to be less in malignant prostate tissue than normal prostate tissue and to be reduced following ARSB silencing and increased following ARSB overexpression in prostate stem cells (22). Treatment with a dominant negative (DN) SHP2 DNA construct significantly increased EGFR expression in the prostate stem cells. In contrast, the constitutively active (CA) SHP2 construct reduced the EGFR (Fig. 1*E*). These findings further implicate SHP2 in mediating the effect of ARSB on EGFR expression.

Binding of biotinylated C4S with SHP2 by ELISA

The SHP2 activity in the prostate stem and epithelial cells was significantly reduced when ARSB was silenced and was

Table 2
Sulfated glycosaminoglycans, chondroitin 4-sulfate, and chondroitin 6-sulfate in prostate cells by the Blyscan assay
Results shown are the mean ± S.D. See Refs. 17 and 22.

	Control		Control siRNA		ARSB siRNA		Vector control		ARSB Overexpressed	
	Stem cells	Epithelial cells	Stem cells	Epithelial cells	Stem cells	Epithelial cells	Stem cells	Epithelial cells	Stem cells	Epithelial cells
	μg/mg protein		*μg/mg protein*		*μg/mg protein*		*μg/mg protein*		*μg/mg protein*	
Total sulfated GAGs	19.2 ± 0.8	18.2 ± 0.2	19.4 ± 0.8	18.6 ± 0.3	25.5 ± 0.9	24.6 ± 0.6	19.5 ± 0.9	18.2 ± 0.5	14.0 ± 0.5	12.2 ± 0.9
C4S[a]	8.0 ± 0.7	8.6 ± 0.2	8.2 ± 0.4	8.7 ± 0.3	14.0 ± 0.2	14.2 ± 0.5	8.3 ± 0.8	8.6 ± 0.4	2.4 ± 0.2	2.6 ± 0.2
C6S[b]	5.1 ± 0.3	4.1 ± 0.3	5.2 ± 0.5	4.1 ± 0.2	5.5 ± 0.7	4.0 ± 0.2	5.1 ± 0.3	4.2 ± 0.2	5.8 ± 0.3	4.0 ± 0.2

[a] Following immunoprecipitation with C4S antibody.
[b] Following immunoprecipitation with C6S antibody.

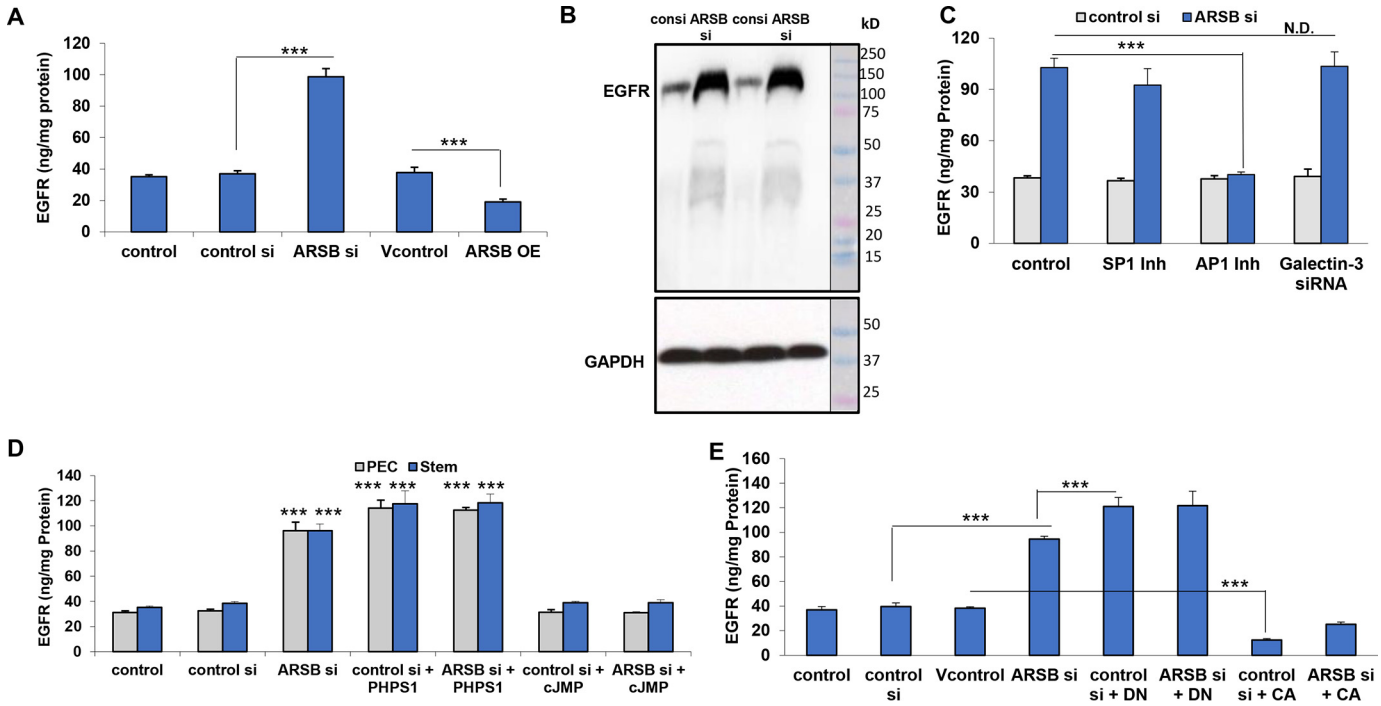

Figure 1. EGFR is increased following decline in ARB or SHP2 and reduced by AP-1 inhibition but unaffected by galectin-3 silencing. *A*, in human prostate stem cells, ARSB siRNA increased EGFR to ~2.8 times the baseline level of 35.2 ± 1.1 ng/mg of protein ($p < 0.001$, one-way analysis of variance with Tukey–Kramer post-test; $n = 3$). Inversely, ARSB overexpression reduced the EGFR to 19.0 ± 1.9 ng/mg of protein ($p < 0.001$; $n = 3$). *B*, representative Western blotting shows the increase in density of EGFR in the prostate stem cells following ARSB silencing. Glyceraldehyde-3-phosphate dehydrogenase (GAPDH) is used as a control. Minimal EGFR degradation is evident. *C*, the increase in EGFR protein caused by ARSB silencing was blocked by inhibition of AP-1 (SR11302; 5 μM for a 2-h pretreatment and then 24 h). In contrast, galectin-3 silencing by siRNA or inhibition of SP1 nuclear binding by mithramycin (250 nM for 24 h) had no effect on the ARSB siRNA- induced increase in EGFR. *D*, EGFR expression was increased by ARSB siRNA or by the SHP2 inhibitor PHPS1 (30 μM for 24 h) in prostate epithelial cells and prostate stem cells ($p < 0.001$; $n = 3$). The increase following PHPS1 was greater than the increase following ARSB silencing ($p < 0.001$). cJMP (400 μM for a 2-h pretreatment and then 24 h) inhibited the ARSB silencing-induced increase, consistent with the observed effect of AP-1 inhibition shown in *C*. *E*, EGFR expression was increased by ARSB siRNA and further increased by the dominant negative SHP2 DNA construct ($p < 0.001$). The constitutively active SHP2 construct significantly inhibited the EGFR, compared with the vector control ($p < 0.001$; $n = 3$). Findings indicate that the decline in SHP2 mediated the effect of ARSB knockdown on EGFR. *Bars*, mean ± S.D. (*error bars*). *consi*, control siRNA; *PEC*, prostate epithelial cells; *si*, siRNA. ***, $p \leq 0.001$. *N.D.*, no difference.

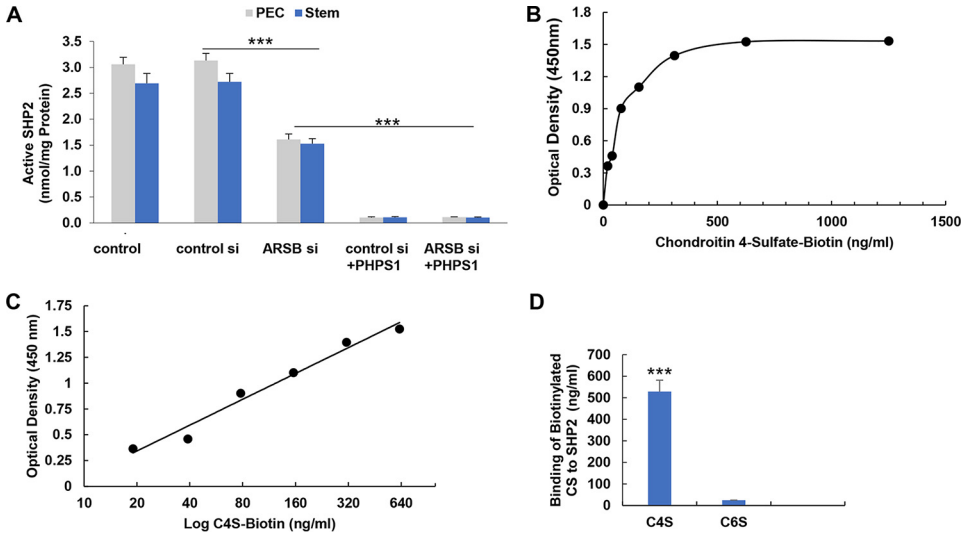

Figure 2. SHP2 activity is reduced following ARSB silencing and is attributable to binding with C4S. *A*, active SHP2 was measured using an exogenous phosphorylated substrate in the prostate stem and epithelial cells. ARSB silencing significantly reduced the SHP2 activity ($p < 0.001$, $n = 3$), and the active SHP2 was further reduced by PHPS1 ($p < 0.001$, $n = 3$). *B*, binding of biotinylated, predominantly C4S chondroitin sulfate to GST-tagged SHP2 (amino acids 246–593), which was coated on the wells of a microtiter plate, peaked at a concentration of 625 ng/ml, based on a standard curve of optical density *versus* concentration of biotinylated, predominantly C4S chondroitin sulfate. *C*, the linear range of the biotinylated C4S ($\log_2$) with GST-tagged SHP2 had slope $m = 0.25$ and y intercept $= -0.74$. *D*, the binding of the biotinylated chondroitin sulfate preparations to GST-tagged SHP2 coated wells was determined using the saturating concentration for C4S of 625 ng/ml. 529.0 ± 52.5 ng/ml of C4S bound to the plate ($p < 0.001$, $n = 3$). In contrast, of 625 ng/ml of predominantly C6S 24.2 ± 1.4 ng/ml bound to the SHP2. These findings demonstrate that the C4S preparation had much higher affinity to bind with SHP2 than C6S. *Bars*, mean value ± S.D. (*error bars*). ***, $p \leq 0.001$.

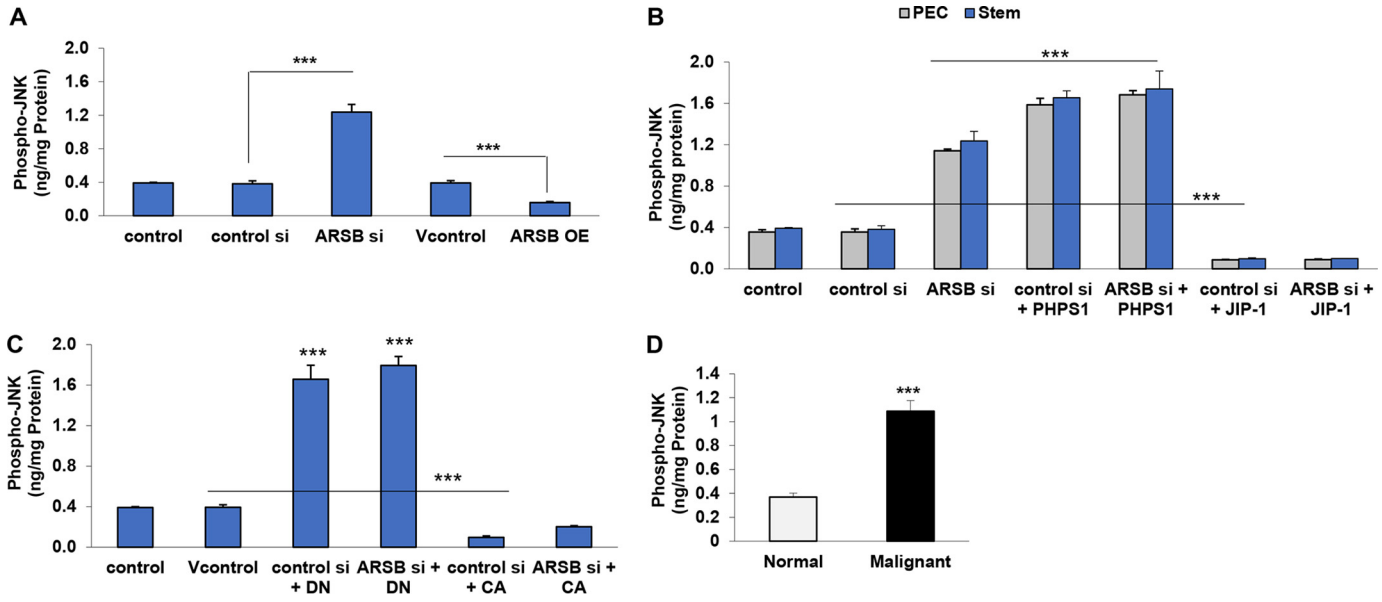

Figure 3. Phospho-JNK is increased in prostate stem cells and prostate tissue following ARSB silencing or SHP2 inhibition. *A*, in prostate stem cells, ARSB silencing significantly increased ($p < 0.001$, $n = 3$) and ARSB overexpression significantly reduced ($p < 0.001$, $n = 3$) the phospho-JNK concentration. *B*, ARSB siRNA significantly increased the phospho-JNK in the prostate epithelial and stem cells ($p < 0.001$, $n = 3$). The SHP2 inhibitor PHPS1 further increased the phospho-JNK levels ($p < 0.001$). JIP-1 significantly reduced phospho-JNK ($p < 0.001$) in the cells. *C*, phospho-JNK was significantly increased by the DN SHP2 construct ($p < 0.001$, $n = 3$) and significantly inhibited by the CA SHP2 in the prostate stem cells ($p < 0.001$, $n = 3$). *D*, in malignant prostate tissue, the phospho-JNK was significantly higher than in the normal prostate tissue ($p < 0.001$, unpaired *t* test, two-tailed, $n = 6$). *Bars*, mean value ± S.D. (*error bars*). ***, $p \leq 0.001$.

reduced further by exposure to PHPS1 (Fig. 2*A*). To determine why SHP2 activity declined when ARSB was reduced, the binding of SHP2 with C4S was addressed by *in vitro*, acellular binding studies. ARSB acts by removing the 4-sulfate group at the nonreducing end of C4S and is required for the degradation of C4S (23–39). The binding of biotinylated, predominantly C4S chondroitin sulfate (86% C4S by disaccharide analysis) with GST-tagged SHP2 (amino acids 246–593) coated on wells of an ELISA plate was determined by measurements of OD. At a C4S concentration of 625 ng/ml, binding was maximal, and no further increase in optical density was obtained with additional C4S ($n = 6$) (Fig. 2*B*). There was a linear response between OD and the log of the concentration of biotinylated C4S from 19 ng/ml to the saturating concentration of 625 ng/ml ($m = 0.25$ and y intercept $t = -0.74$) (Fig. 2*C*). Binding to SHP2 of predominantly C4S was compared with binding of predominantly C6S (96% by disaccharide analysis). SHP2 preferentially bound with C4S (Fig. 2*D*). 529.0 ± 52.5 ng/ml C4S bound to the SHP-2–coated microplate ($p < 0.001$, $n = 3$) when 625 ng/ml was added. 24.2 ± 1.4 ng/ml of C6S bound (Fig. 2*D*). These data indicate that C4S has a significantly greater affinity to bind with SHP2 than C6S and that increasing concentrations of C4S lead to increased binding with SHP2 until the saturating concentration of 625 ng/ml. These experiments indicate that a decline in ARSB with a concomitant increase in C4S can lead to increased binding of C4S with SHP2. In contrast, C6S showed significantly less affinity with SHP2.

Declines in ARSB or SHP2 lead to increased JNK activation

To explain how a decline in SHP2 activity following ARSB silencing could lead to enhanced EGFR mRNA expression, the impact of SHP2 on phospho-JNK activity was evaluated, because inhibition of AP-1 DNA binding reduced EGFR (see Fig. 1*B*). Phospho-JNK increased following ARSB silencing and declined when ARSB was overexpressed in the prostate stem cells (Fig. 3*A*). Treatment with the SHP2 inhibitor PHPS1 increased the phospho-JNK in the stem and epithelial cells, whereas the JNK-selective inhibitor peptide (JIP-1) was inhibitory (Fig. 3*B*). The increase in phospho-JNK was inhibited by the CA SHP2 construct, whereas the DN SHP2 increased the phospho-JNK (Fig. 3*C*). The phospho-JNK was also increased in the malignant prostate tissue, compared with the normal tissue (Fig. 3*D*).

Activation of EGFR promoter following decline in ARSB or SHP2

In the prostate stem cells, the nuclear DNA binding of c-Jun/c-Fos was increased when ARSB was silenced and reduced when ARSB was overexpressed (Fig. 4*A*). Consistent with the impact of ARSB on C4S and SHP2 activity, inhibition of SHP2 had an effect similar to silencing ARSB. When SHP2 was inhibited by the DN construct, the nuclear DNA binding of c-Jun/c-Fos was increased, and the CA SHP2 construct blocked the increase in nuclear DNA c-Jun/c-Fos (Fig. 4*B*). In the prostate epithelial and stem cells, the SHP2 inhibitor PHPS1 further increased the nuclear DNA binding of the AP-1 components beyond the effect of ARSB silencing ($p < 0.001$, $n = 3$). The baseline levels of binding were inhibited by cJMP and JIP-1 ($p < 0.01$, $n = 3$) (Fig. 4*C*).

Analysis of EGFR promoter activation was performed using a luciferase-tagged promoter construct. Promoter activity in the prostate stem cells increased to approximately 3 times the control level, following ARSB silencing, and further increased when treated with PHPS1 (Fig. 4*D*). SR11302, which blocks AP-1

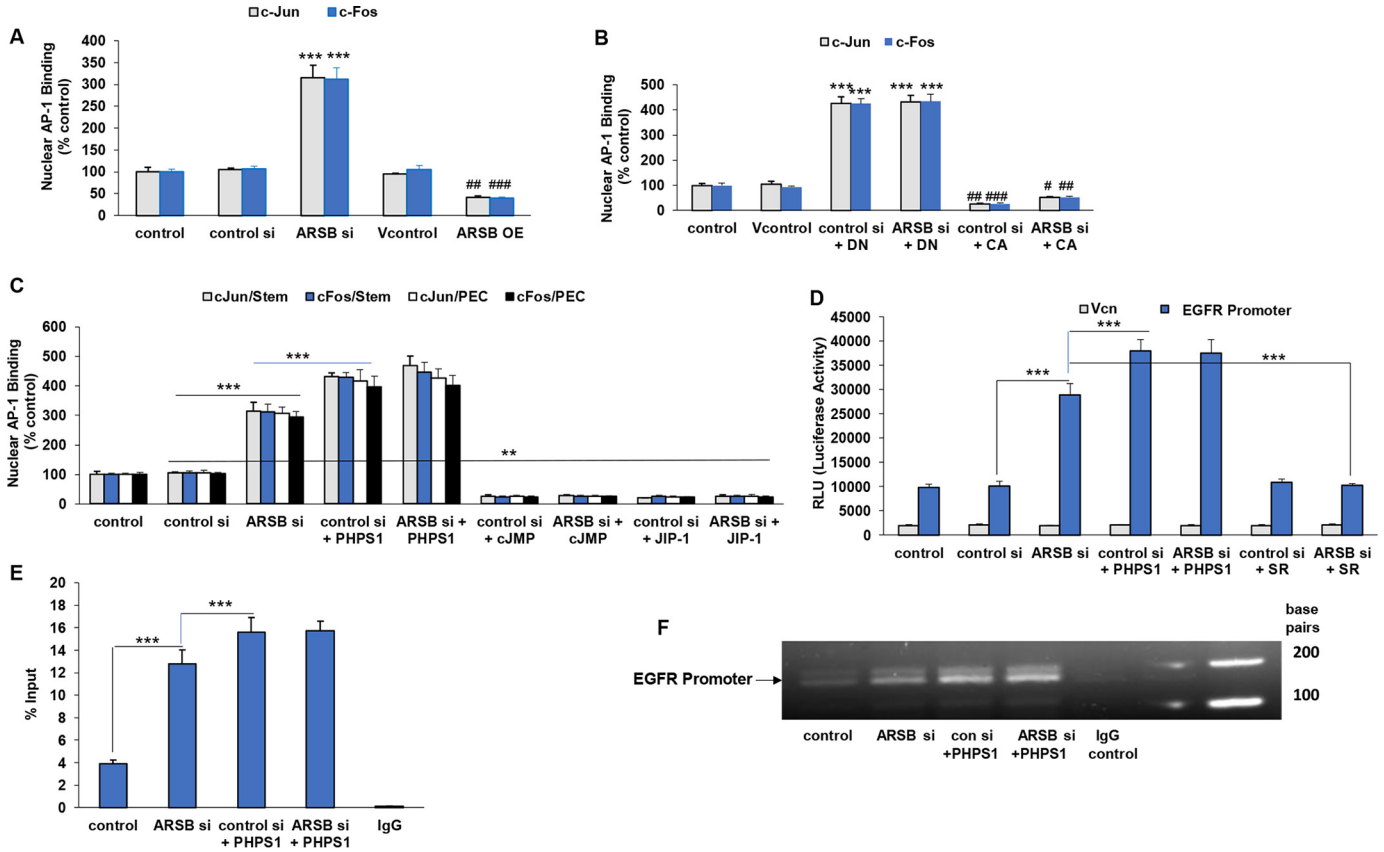

Figure 4. Increased nuclear AP-1 binding and EGFR promoter activation following ARSB silencing or SHP2 inhibition. *A*, nuclear DNA binding of AP-1 components c-Jun and c-Fos were increased in prostate stem cells when ARSB was silenced ($p < 0.001$, $n = 3$) and significantly reduced ($p < 0.01$, $p < 0.001$, $n = 3$) when ARSB was overexpressed. *B*, SHP2 DNA constructs significantly modified the nuclear DNA binding of AP-1 components in the prostate stem cells. DN SHP2 increased c-Jun and c-Fos ($p < 0.001$, $n = 3$), and CA reduced the binding ($p < 0.01$, $p < 0.001$, $n = 3$). *C*, the SHP2 inhibitor PHPS1 further increased the nuclear AP-1 binding compared with the ARSB silencing–induced increase ($p < 0.001$, $n = 3$). cJMP and JIP-1 significantly reduced the binding from the baseline levels in the prostate stromal and epithelial cells ($p < 0.01$, $n = 3$). *D*, both ARSB silencing and SHP2 inhibition markedly increased the EGFR promoter activation in prostate stem cells ($p < 0.001$, $n = 5$). SR11302, the AP-1 inhibitor, reduced the effect of ARSB silencing to baseline level ($p < 0.001$, $n = 5$). *E*, a ChIP assay showed the effects of ARSB silencing and the PHPS1 inhibitor on the DNA binding to the EGFR promoter ($p < 0.001$, $n = 5$). *F*, agarose gel showed the increased intensity of the EGFR promoter band following ARSB silencing or treatment with PHPS1. PHPS1 had greater effect than ARSB silencing. *Bars*, mean value ± S.D. (*error bars*). *** or ###, $p \leq 0.001$; ** or ##, $p \leq 0.01$; #, $p \leq 0.05$.

nuclear binding, inhibited the ARSB knockdown–induced increase in promoter activation (Fig. 4*D*). By a chromatin immunoprecipitation (ChIP) assay, the DNA bound to the EGFR promoter was significantly increased following ARSB silencing or by PHPS1 treatment (Fig. 4*E*). The accompanying blot demonstrates the increased density of binding to the EGFR promoter DNA following ARSB silencing or PHPS1 treatment (Fig. 4*F*).

EGFR binding with C4S in prostate stem cells

Binding of exogenous EGF to the prostate stem cells increased when ARSB was silenced ($p < 0.001$, $n = 3$) and declined when ARSB was overexpressed ($p < 0.001$, $n = 3$) (Fig. 5*A*). In response to exogenous EGF, the 5-bromo-2′-deoxyuridine (BrdU) incorporation in the prostate stem cells increased when ARSB was silenced (Fig. 5*B*). These findings suggest that the transcriptional effects of ARSB on EGFR may lead to enhanced cell proliferation in response to EGF due to increased availability of EGFR.

Overall pathway from ARSB to increase in EGFR expression

The overall signaling pathway from decline in ARSB and the associated increase in C4S is depicted (Fig. 6). The decline in SHP2 activity is due to enhanced binding with C4S, leading to the sustained phosphorylation of JNK and the activation of c-Jun/c-Fos. The increased binding of the AP-1 components to the EGFR promoter stimulates EGFR mRNA expression. Exposure to exogenous EGF leads to increased BrdU incorporation, consistent with enhanced cell proliferation.

Discussion

Regulation of EGFR expression is critically important in the control of cell proliferation and differentiation. The experiments in this report show that decline in the enzyme ARSB and the associated increase in chondroitin 4-sulfate lead to inhibition of SHP2 activity, with resultant increased activation of JNK. JNK phosphorylation leads to increased nuclear DNA binding of c-Jun and c-Fos. These components of AP-1 bind to the EGFR promoter, leading to increased expression of EGFR in the prostate cells. The increased protein may reflect reduced protein turnover as well as increased expression in the prostate cells. These findings demonstrate how sulfatase regulation of phosphatase activity can have a profound impact on signaling cascades in human cells and can regulate vital transcriptional events. Because ARSB activity is modifiable by variation in ambient conditions, including oxygen and chloride (20, 29),

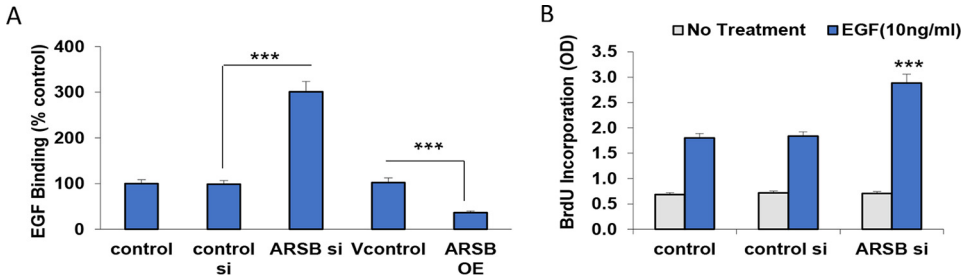

Figure 5. Increased BrdU incorporation in prostate stem cells in response to exogenous EGF following ARSB silencing. *A*, exogenous EGF binding to the prostate stem cells significantly increased when ARSB was silenced and declined when ARSB was overexpressed. *B*, the BrdU incorporation increased significantly following exposure to exogenous EGF when ARSB was silenced, consistent with increased availability of EGFR-binding sites when EGFR expression was increased. *Bars*, mean value ± S.D. (*error bars*). ***, $p \leq 0.001$.

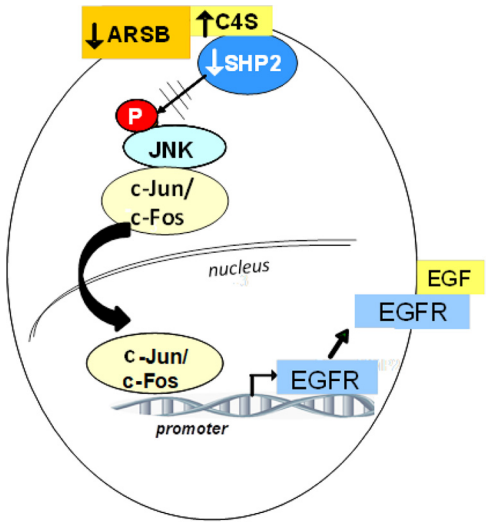

Figure 6. Overall schematic to show how decline in ARSB and the accompanying increase in C4S lead to increased expression of EGFR. Increased C4S binds more SHP2, inhibiting the phosphatase activity, leading to increased phospho-JNK and increased nuclear DNA binding of the AP-1 components c-Fos and c-Jun and activation of the EGFR promoter. *Bars*, mean value ± S.D. (*error bars*).

changes in ARSB activity provide an opportunity for subtle, specific effects on chondroitin sulfation and chondroitin 4-sulfate binding with critical molecules, such as SHP2. Inhibition of phosphatase activity can lead to sustained effects on downstream phosphorylations, including phospho-ERK (19, 22), phospho-p38 (21), and phospho-JNK.

The role of SHP2 inhibition in malignancy is controversial, with some reports indicating that SHP2 is a proto-oncogene and its inhibition is beneficial (30–36). Other reports indicate enhanced malignant potential when SHP2 is inhibited, leading to sustained tyrosine phosphorylations (19, 21, 37–40). In this report, ARSB silencing and inhibition of SHP2 lead to increased phospho-JNK, activation of the JNK targets c-Jun and c-Fos, activation of the EGFR promoter, and increased EGFR expression. This pathway may explain the previously observed increase in EGFR in malignant prostate tissue and prostate cells. When ARSB activity is reduced and C4S is thereby increased, the C4S chains attached to proteoglycans may sterically hinder the binding of EGF-like motifs of proteoglycans, such as those of versican, with EGFR on cell surfaces. The binding of exogenous EGF with EGFR may increase. In response to exogenous EGF following ARSB silencing, BrdU incorporation increased, demonstrating functional EGFR. These results present a vital role for EGFR in the response of prostate cells following decline in ARSB. The current studies have demonstrated a pathway by which the decline in ARSB can lead to an increase in EGFR and may subsequently impact cell proliferation.

The acellular C4S-SHP2 binding experiments show preferential binding of C4S with SHP2, rather than C6S. When the SHP2 inhibitor PHPS1 was developed, the SHP2/PHPS1-binding model demonstrated that the phenyl sulfonate group of PHPS1 acted as a phosphotyrosine mimetic (41). The sulfonate group penetrated into the substrate-binding pocket of SHP2. The current experiments suggest that the sulfate group of GalNAc 4-sulfate of C4S may also act as a phosphotyrosine mimetic and penetrate into the substrate binding pocket of SHP2. The amino acids at the periphery of the cleft where the PHPS1 sulfate binds are Lys-280, Asn-281, Arg-362, and His-426. These residues, which are distinct in SHP2, may stabilize the anionic sulfate of C4S and maintain SHP2 in an inactive conformation. The 4-sulfate group of C4S may represent a unique configuration, as it has previously been shown to be critically important in binding of malarial parasites in the vasculature (42).

In addition to versican, several other proteoglycans have been identified on the cell surface or in the stroma of normal or malignant prostate. These include the small leucine-rich proteoglycans, decorin, biglycan, lumican, and fibromodulin. Decorin and biglycan may have dermatan sulfate attachments that are modified by ARSB, and the accumulation of dermatan sulfate may also affect signaling pathways in prostate and in other tissues. In contrast, the keratan sulfate attachments of lumican and fibromodulin would be unaffected by changes in ARSB. Of these, decreases of decorin and lumican have been shown in prostate tumors (43). Other lecticans, including aggrecan and brevican, and proteoglycans with heparan sulfate attachments, including syndecan-1, perlecan, betaglycan, and glypican-1 have also been identified in prostate tissues (44–48). Differential expression of versican isoforms has been identified in malignant brain tumors, with the V2 isoform, which has the α-GAG attachment site, predominant in normal brain and in glioma extracellular matrix (49). In melanoma cells, V3 overproduction was shown to reduce the tumorigenicity (50), and V3 overexpression reduced interaction with CD44 and impacted ERK1/2 and p38 mitogen-activated protein kinase signaling pathways (51). Further characterization of the impact of specific versican domains and of versican degradation prod-

ucts in prostate cancers may help to explain how the chondroitin sulfate attachments on versican affect cell signaling and proliferation. Versican proteolysis by ADAMTS proteases or matrix metalloproteases is anticipated to influence how the versican-associated chondroitin sulfate chains can interact with the versican EGF-like motifs, as well as how other specific versican regions impact cell signaling and proliferation (52, 53).

Prior reports have noted that androgens down-regulate EGFR in normal prostate, but not in prostate cancer, and loss of EGFR regulation may contribute to the transition from androgen dependence to androgen independence (3, 12). The activation of the HER-kinase axis appears to enable progression of prostate cancer to androgen-independence, suggesting a convergence of the lost effect of androgen on EGFR expression and the activation of the HER-kinase axis with androgen independence (13). Further consideration of the roles of ARSB, C4S, and SHP2 in the expression of EGFR and in the sustained activation of phosphorylation targets may help to clarify the underlying mechanisms that cause the transition from hormone dependence to hormone independence.

Experimental procedures

Cell culture of prostate cells

Human prostate epithelial cells (ATCC®, CRL-2850™) and human prostate stem (CRL-2887) cell lines were obtained from the American Type Culture Collection (ATCC, Manassas, VA). The cells were grown in keratinocyte serum-free medium with 0.05 mg/ml bovine pituitary extract and 5 ng/ml EGF and maintained at 37 °C in a humidified, 5% CO_2 environment with new medium every third day, as described previously (17, 22). Confluent cells in T-25 flasks were harvested by EDTA-trypsin and subcultured in multiwell tissue culture plates under similar conditions to perform the experiments that are presented in this report.

Human prostate tissue

Frozen tissue samples from radical prostatectomies performed for prostate cancer ($n = 9$) were obtained from the University of Illinois at Chicago Tissue Bank under a protocol approved by the institutional review board of the University of Illinois at Chicago and the Cancer Center of the University of Illinois. Frozen sections were performed, and benign and malignant foci, consisting of epithelium and stroma, were identified, isolated, dissected, and frozen for subsequent analysis, as described previously (15).

Measurement of ARSB (GalNAc-4-sulfatase) activity and chondroitin sulfates

ARSB activity in the control and treated cells was determined using 4-methylumbelliferyl sulfate (Sigma) as substrate (15). Total sulfated glycosaminoglycans, including heparin, heparan sulfate, dermatan sulfate, chondroitin 4-sulfate, chondroitin 6-sulfate, and keratan sulfate, were measured by the sulfated GAG assay (Blyscan™, Biocolor Ltd., Newtownabbey, Northern Ireland) (15). The Blyscan assay uses 1,9-dimethylmethylene blue to detect sulfated polysaccharides and does not detect disaccharides or hyaluronan. Detection of DNA is minimal at the assay pH of 1.7. Chondroitin 4-sulfate was immunoprecipitated from the cell lysates by specific chondroitin 4-sulfate antibody (Ly111, Amsbio, Cambridge, MA), a purified mouse mAb/IgM, κ-chain, and then measured by the Blyscan assay kit (54, 55). Chondroitin 6-sulfate was immunoprecipitated from the cell lysates by specific mouse monoclonal IgM chondroitin 6-sulfate antibody (clone MC21C, LS-C79286, LSBio, Seattle, WA) and quantified by the Blyscan assay, as stated above.

To test the recovery and specificity of CS chains detected by the CS antibodies, a standard OD curve using known quantities of C4S (Blyscan) was prepared. Magnetic beads were coated with 2 μg of either LY111 or MC21C antibody, and the recovery of C4S and C6S from bovine trachea or shark cartilage chondroitin sulfate samples was determined by the Blyscan assay, based on the known percentage of C4S or C6S determined by the disaccharide analysis (see below). The recovery of C4S by the Ly111 antibody was 96.5 ± 3.2% (corresponding to 1.64 ± 0.05 μg and 86% C4S, $n = 3$). The recovery of the C6S by the MC21C antibody was 95.3 ± 3.0% (corresponding to 1.39 ± 0.04 μg and 73% C6S, $n = 3$).

Arylsulfatase B and galectin-3 silencing by siRNA

Specific siRNAs for ARSB (NM_000046) and galectin-3 (Hs_LGALS3_9) and control siRNAs were procured (Qiagen, Valencia, CA), and ARSB and galectin-3 were silenced (17). Effectiveness of silencing was confirmed by an ARSB activity assay or by galectin-3 ELISA (R&D Systems, Bio-Techne, Minneapolis, MN).

Arylsulfatase B and SHP-2 transfections

ARSB plasmid in pCMV6-XL4 vector was obtained (Origene) and overexpressed in prostate stem/epithelial cells by transient transfection using 2 μg of the plasmid and Lipofectamine™ 2000 (22, 55). Controls included untransfected cells and cells transfected with ARSB vector control. Media were changed after 6 h, and cells were incubated in a humidified, 37 °C, 5% CO_2 environment and then harvested 24 h after transfection. Effectiveness was determined by measuring ARSB activity. SHP-2 dominant negative, constitutively active, WT and empty vector plasmids were obtained (from Dr. Stuart Frank, University of Alabama at Birmingham) (56) and transfected in the prostate stem cells by Lipofectamine™ 2000. The efficiency of transfection was determined by measuring SHP2 activity (21).

Disaccharide analysis of chondroitin sulfates

Each CS sample was resuspended to 10 μg/μl; 100 ng was used for GAG analysis. The total GAG amounts reported in this report refer to the total GAG per sample vial we received.

Unsaturated disaccharide standards of CS

ΔUA-GalNAc; ΔUA-GalNAc4S; ΔUA-GalNAc6S; ΔUA2S-GalNAc; ΔUA2S-Gal-NAc4S; ΔUA2S-GalNAc6S; ΔUA-GalNAc4S6S; ΔUA2S-GalNAc4S6S), unsaturated disaccharide standards of HS ΔUA-GlcNAc; ΔUA-GlcNS; ΔUA-GlcNAc6S; ΔUA2S-GlcNAc; ΔUA2S-GlcNS; ΔUA-GlcNS6S; ΔUA2S-GlcNAc6S; ΔUA2S-GlcNS6S), and unsaturated disaccharide

standard of HA (ΔUA-GlcNAc), where ΔUA is 4-deoxy-α-L-threo-hex-4-enopyranosyluronic acid, were purchased from Iduron (Macclesfield, UK). Actinase E was obtained from Kaken Biochemicals (Tokyo, Japan). Chondroitin lyase ABC from *Proteus vulgaris* was expressed in in our laboratory. Recombinant flavobacterial heparin lyases I, II, and III were expressed in our laboratory using *Escherichia coli* strains provided by Jian Liu (College of Pharmacy, University of North Carolina). 2-Aminoacridone (AMAC) and sodium cyanoborohydride were obtained from Sigma-Aldrich. All other chemicals were of HPLC grade. Vivapure Q Mini H strong anion exchange spin columns were from Sartoriou Stedim Biotech (Bohemia, NY).

The digestion was performed in a 3,000 molecular weight cutoff spin column, and 300 μl of digestion buffer (50 mM ammonium acetate containing 2 mM calcium chloride adjusted to pH 7.0) was added to the filter unit. Recombinant heparin lyase I, II, and III (pH optima 7.0–7.5) and recombinant chondroitin lyase ABC (10 millunits each, pH optimum 7.4) were added to each sample and mixed well. The samples were all placed in a water bath at 37 °C for 12 h, after which enzymatic digestion was terminated by removing the enzymes by centrifugation. The filter unit was washed twice with 250 μl of distilled water, and the filtrates containing the disaccharide products were dried via vacuum centrifuge.

Half of the dried samples were AMAC-labeled by adding 10 μl of 0.1 M AMAC in DMSO/acetic acid (17:3, v/v), incubating at room temperature for 10 min, followed by adding 10 μl of 1 M aqueous sodium cyanoborohydride and incubating for 1 h at 45 °C. A mixture containing all 17 disaccharide standards prepared at 0.5 ng/μl was similarly AMAC-labeled and used for each run as an external standard. After the AMAC-labeling reaction, the samples were centrifuged, and each supernatant was recovered.

LC was performed on an Agilent 1200 LC system at 45 °C using an Agilent Poroshell 120 ECC18 (2.7 μm, 3.0 × 50 mm) column. Mobile phase A (MPA) was 50 mM ammonium acetate aqueous solution, and the mobile phase B was methanol. The mobile phase passed through the column at a flow rate of 300 μl/min. The gradient was 0–10 min, 5–45% B; 10–10.2 min, 45–100% B; 10.2–14 min, 100% B; 14–22 min, 100–5% B. Injection volume was 5 μl.

A triple-quadrupole MS system equipped with an electrospray ionization source (Thermo Fisher Scientific, San Jose, CA) was used a detector. The online MS analysis was in the multiple-reaction monitoring mode. MS parameters were as follows: negative ionization mode with a spray voltage of 3000 V, a vaporizer temperature of 300 °C, and a capillary temperature of 270 °C.

Biotinylation of chondroitin sulfates

Two different chondroitin sulfates, chondroitin sulfate C from shark cartilage (predominantly C6S; Seikagaku, Tokyo, Japan) and chondroitin sulfate A from bovine trachea (predominantly C4S; Sigma) were procured. Disaccharide analysis of chondroitin sulfate C from shark (see above) cartilage revealed 73% 6S, 19 ± 1% 4S, 8% 2S6S, and 1% 0S. Disaccharide analysis of chondroitin sulfate A from bovine trachea showed 86 ± 1% C4S, 12 ± 1% C6S, and 2% C0S. These chondroitin sulfates were biotinylated using established methods (57). 1.14 mg of chondroitin sulfate, 1.88 mg of EZ Link-Hydrazide-PEG_4-Biotin (Thermo Scientific, Waltham, MA), and 1.2 mg of sodium cyanoborohydride (NaBH3CN; Sigma) were dissolved in 170 μl of H_2O. 30 μl of acetic acid (AcOH) was added to the mixture, which was incubated at 70 °C for 2 days with mixing. Additional portions of NaBH3CN (1.2 mg) and 1.88 mg of EZ Link-Hydrazide-PEG_4-biotin were added after 24 h. At 48 h, the mixture was desalted by passing through a spin column (1000 molecule weight cut-off). The yield of biotinylated chondroitin sulfate was determined by the Blyscan™ assay and was 93.8% for predominantly C4S and 95.4% for predominantly C6S.

Assay for binding of chondroitin sulfate with SHP2 (PTPN11)

Microtiter plates were coated with GSH-*S*-transferase (GST) (PTPN11) antibody (ab18183; Abcam, Cambridge, MA) by incubating 100 μl (2 μg/ml in PBS) of antibody solution in each well at RT overnight. After coating, wells were washed three times with PBS, pH 7.4, with 0.05% Tween 20. Then preparations were blocked for 1 h at RT with blocking buffer (PBS, pH 7.4, with 1% BSA). After blocking, 100 μl of (0.5 μg/ml) PTPN11-GST (Creative Biomart, Shirley, NY) in PBS was added to each well. Plates were incubated at RT for 2 h and then washed three times with wash buffer. The binding curve for C4S with GST-tagged SHP2 was determined using 50 μl at concentrations ranging from 0.019 to 1.25 μg/ml. Binding was saturated at a concentration of 625 ng/ml. The three biotinylated chondroitin sulfates were added at a concentration of 625 ng/ml to the wells of the microtiter plate. The plates were incubated at RT for 2 h and then washed, and 100 μl of 1:200 Streptavidin-HRP was added to each well. Plates were incubated at RT for 20 min and washed. Next, 100 μl of color reagent (1:1 substrate A and B) was added, and plates were incubated at RT for 15 min. The reaction was stopped with 50 μl of Stop Solution-2 N H_2SO_4 and read at 450 nm in a plate reader. The amount of biotinylated chondroitin sulfate that bound to the PTPN11-GST was determined by the OD measurements. For the displacement assay, 50 μl of 1.25 μg/ml of biotinylated C4S and 50 μl of 1.25–6.25 μg/ml of unlabeled C4S or C4S-C6S combination were added to each well, and the OD (binding) was detected for each concentration of the unlabeled chondroitin sulfate (58).

SHP-2 activity assay

SHP-2 activity in control and treated prostate stem cells and epithelial cells or in the control and malignant prostate tissue was measured by a commercial SHP-2 Duo Set IC activity assay (R&D Systems, Bio-Techne). In this assay, SHP2 molecules were immunoprecipitated by an anti-SHP-2 antibody conjugated to agarose beads. After washing away unbound material, a synthetic phosphopeptide substrate was added to the immunoprecipitates. Substrate was dephosphorylated by active SHP-2 in the sample to generate free phosphate and unphosphorylated peptide. The amount of free phosphate in the supernatant was detected by a sensitive dye-binding assay using malachite green and molybdic acid. The activity of SHP-2 was

determined from the phosphate standard curve. Cell preparations were treated with phenylhydrazonopyrazolone sulfonate (PHPS1), an SHP2 inhibitor (30 μM for 24 h; Sigma) to inhibit SHP2 activity (21, 51).

Phospho-JNK ELISA

Cell extracts were prepared from both treated and control prostate stem and epithelial cells in cell lysis buffer. Malignant or control prostate tissue was homogenized for the measurement of phospho-JNK. Phospho-JNK was measured in cell and tissue samples using a DuoSet sandwich ELISA kit (R&D Systems, Bio-Techne). Samples and standards were added to the wells of the microtiter plate precoated with a capture antibody to human JNK. Phospho-JNK in the lysates was captured by the coated antibody on the plate and detected with biotinylated antibody to phospho-JNK. Streptavidin-HRP and hydrogen peroxide/tetramethylbenzidine substrate were used to develop color proportional to the bound HRP activity. The reaction was stopped, and the optical density of the color was read at 450 nm in a plate reader (FLUOstar, BMG, Cary, NC). Phospho-JNK concentrations in the samples were extrapolated from a curve derived using known standards.

Oligonucleotide-based ELISA to detect nuclear c-Jun and c-Fos

Binding of c-Jun and c-Fos to the AP-1 binding site in the nuclear DNA was measured by an oligonucleotide-binding assay (TransAM kit, Active Motif, Carlsbad, CA). Nucleus-bound c-Jun and c-Fos in the prostate stem and epithelial cells following ARSB silencing or ARSB overexpression and in normal and malignant prostate tissue were determined as per the instructions. Nuclear extracts were prepared using a nuclear extract preparation kit (Active Motif) and were added to the wells of a 96-well microtiter plate, precoated with the AP-1 consensus oligonucleotide sequence 5′-TGAGTCA-3′. Sample values were normalized by total cell protein and expressed as a percentage of untreated control. Nuclear c-Jun and c-Fos in normal and malignant prostate tissue were also determined by the same assay.

Inhibition of JNK, c-Jun phosphorylation, and c-Fos binding to DNA

To further investigate the role of JNK and the transcription factors c-Jun and c-Fos on EGFR promoter activation, prostate cells were exposed to specific inhibitors. These included the cell-permeable cJMP (ILKQSMTLNLADPVGSLKPHLRAKN; 400 μM for a 2-h preincubation for total of 26 h; R&D Systems, Bio-Techne), which prevents JNK/c-Jun interaction and the phosphorylation of c-Jun (59); a JNK-selective inhibitor peptide based on residues 153–163 of JIP-1 (RPKRPTTLNLF-NH_2; 10 μM for a 2-h preincubation for total of 26 h; Tocris, Bio-Techne) (60); and SR11302 (5 μM for a 2-h pretreatment for a total of 26 h; Santa Cruz Biotechnology, Inc.), a synthetic retinoid that inhibits AP-1 transcription factor activity by blocking binding of c-Fos to the AP-1 consensus sequence (61). Prostate cells were treated with cJMP, JIP-1, c-Fos–DNA binding inhibitor (SR11302), SHP2 inhibitor (PHPS1), or SHP-2 DN or CA DNA constructs, and effects on EGFR expression, promoter activation, and nucleus-bound c-Jun and c-Fos were determined.

ELISA and Western blotting for EGFR

EGFR protein was quantified following ARSB silencing and overexpression, galectin-3 silencing, and transfection of SHP-2 dominant negative and constitutively active plasmid DNA in prostate stem cells. EGFR protein was also measured in the prostate stem and/or epithelial cells after treatment with the SHP2 inhibitor PHPS1 (51), the AP-1 DNA binding inhibitor SR11302 (61), cJMP (59), and Sp1 DNA binding inhibitor (mithramycin A; 250 nM for 24 h) (62). Total EGFR protein was determined using commercial ELISA DuoSet (R&D Systems, Bio-Techne), as described previously (15). EGFR Western blotting was performed using EGFR antibody (AF231, R&D Systems, Bio-Techne) with glyceraldehyde-3-phosphate dehydrogenase control antibody (SCBT, Santa Cruz Biotechnology) for equal loading on a 10% SDS gel, using established methods. Immunoreactive bands were visualized using enhanced chemiluminescence (GE Healthcare).

Detection of EGFR promoter activity by luciferase reporter assay

EGFR promoter activity following ARSB silencing and treatment with the SHP2 inhibitor (PHPS1) and the AP-1 DNA binding inhibitor (SR11302) was determined by a human EGFR promoter construct in a *Renilla reniformis* luciferase reporter gene (Ren SP). The changes in luminescence due to modifications in binding to the EGFR promoter were detected by the LightSwitch assay system (SwitchGear Genomics, Menlo Park, CA). The β-actin promoter (GoClone) construct was a positive control, and a scrambled sequence (R01) with the *Renilla* luciferase reporter was a negative control, and they were used to determine the effectiveness of transcription and specificity of the reactions. Transfections were performed with cells at 70% confluence, following silencing for 24 h, using FuGENE HD transfection reagent with proprietary LightSwitch assay reagent (SwitchGear). After incubation for 24 h, luminescence was read at 480 nm in a microplate reader (BMG).

AP-1 binding to EGFR promoter assessed by a ChIP assay

For the ChIP assay, ARSB-silenced and control-silenced prostate stem cells were treated with SHP2 inhibitor PHPS1 (30 μM for 24 h) and then fixed with 1% formaldehyde for 10 min at room temperature. This was followed by shearing of chromatin by sonication (ChIP assay, Active Motif, Carlsbad, CA). Sheared DNA was incubated with specific antibody for 1 h as well as with IgG control. Protein-DNA complexes were precipitated by protein A/G-coupled magnetic beads. DNA was purified from the immunoprecipitated complexes by reversal of cross-linking, followed by proteinase K treatment. Then real-time RT-PCR was performed using the following primers for the EGFR promoter (left, 5′-ACGACAGGCCACCTCGTC-3′; right, 5′-TTTCCTCCAGAGCCCGACT-3′). They encompassed the consensus sequence CCCCTGACTCCG, which is the binding site for the AP-1 transcription factor. Band intensity was compared among the ARSB-silenced, inhibitor

(PHPS1)-treated, control-silenced, and IgG control samples on a 1.5% agarose gel.

Binding of exogenous EGF with EGFR

ARSB was silenced or overexpressed in cultured prostate stem cells. After ARSB silencing or overexpression for 24 h, the stem cells were deprived of exogenous EGF for 12 h. Cells were thoroughly washed and challenged with fresh media containing EGF-Biotin (Thermo Fisher) and incubated for 1 h. Cells were washed with wash buffer three times, and then Streptavidin-HRP conjugate was added for 20 min at room temperature. Cells were washed again three times with wash buffer, and the bound EGF was quantified by adding the chromogenic substrate hydrogen peroxide and tetramethylbenzidine. Finally, color development due to HRP activity was stopped by 2 N sulfuric acid. Intensity of color was measured at 450 nm in a plate reader (BMG).

BrdU ELISA to measure cell proliferation

Cell proliferation was quantified by measurement of BrdU incorporation during DNA synthesis in the prostate stem cells. BrdU incorporation was measured by a commercial BrdU cell proliferation assay kit (Cell Signaling Technology, Inc., Danvers, MA) (17). Before EGF challenge, prostate stem cells were deprived of any EGF in the media for 12 h and then challenged with exogenous EGF (10 ng/ml for 24 h).

Statistics

Statistical significance was determined by one-way analysis of variance followed by post hoc Tukey's test for multiple determinations using InStat3 software (GraphPad, La Jolla, CA), unless stated otherwise. Unpaired *t* tests, two-tailed, were used for other comparisons. In the figures with bar graphs, values are expressed as the mean ± S.D. p values ≤ 0.05 are considered statistically significant: *** or ###, $p \leq 0.001$; ** or ##, $p \leq 0.01$; # or *, $p \leq 0.05$.

Author contributions—S. B. and J. K. T. conceived and designed the overall study and wrote the manuscript with the help of L. F., F. Z., and R. J. L. X. H. and Y. O. performed the disaccharide analysis, and S. B. and L. F. performed the other experiments. All authors reviewed the results and approved the final version of the manuscript.

Acknowledgments—We acknowledge the contribution of study materials from Dr. Stuart Frank (University of Alabama at Birmingham) and the contribution of Grace Guzman, M.D. (Department of Pathology) to dissection of malignant and normal prostate tissue.

References

1. Ching, K. Z., Ramsey, E., Pettigrew, N., D'Cunha, R., Jason, M., and Dodd, J. G. (1993) Expression of mRNA for epidermal growth factor, transforming growth factor-α, and their receptor in human prostate tissue and cell lines. *Mol. Cell. Biochem.* **126,** 151–158 CrossRef Medline
2. Sherwood, E. R., and Lee, C. (1995) Epidermal growth factor-related peptides and the epidermal growth factor receptor in normal and malignant prostate. *World J. Urol.* **13,** 290–296 Medline
3. Herbst, R. S. (2004) Review of epidermal growth factor receptor biology. *Int. J. Radiat. Oncol. Biol. Phys.* **59,** 21–26 CrossRef Medline
4. Guérin, O., Fischel, J. L., Ferrero, J. M., Bozec, A., and Milano, G. (2010) EGFR targeting in hormone-refractory prostate cancer: current appraisal and prospects for treatment. *Pharmaceuticals* **3,** 2238–2247 CrossRef Medline
5. Olayioye, M. A., Neve, R. M., Lane, H. A., and Hynes, N. E. (2000) The ErbB signaling network: receptor heterodimerization in development and cancer. *EMBO J.* **19,** 3159–3167 CrossRef Medline
6. Di Lorenzo, G., Autorino, R., De Laurentiis, M., Cindolo, L., D'Armiento, M., Bianco, A. R., and De Placido, S. (2004) HER-2/neu receptor in prostate cancer development and progression to androgen independence. *Tumori* **90,** 163–170 CrossRef Medline
7. Jathal, M. K., Chen, L., Mudryj, M., and Ghosh, P. M. (2011) Targeting ErbB3: the new RKD(id) on the prostate cancer block. *Immunol. Endocr. Metab. Agents Med. Chem.* **11,** 131–149 CrossRef Medline
8. Seth, D., Shaw, K., Jazayeri, J., and Leedman, P. J. (1999) Complex post-transcriptional regulation of EGF-receptor expression by EGF and TGF-α in human prostate cancer cells. *Br. J. Cancer* **80,** 657–669 CrossRef Medline
9. van der Veeken, J., Oliveira, S., Schiffelers, R. M., Storm, G., van Bergen En Henegouwen, P. M., and Roovers, R. C. (2009) Crosstalk between epidermal growth factor receptor- and insulin-like growth factor-1 receptor signaling: implications for cancer therapy. *Curr. Cancer Drug Targets* **9,** 748–760 CrossRef Medline
10. Kovacs, E., Zorn, J. A., Huang, Y., Barros, T., and Kuriyan, J. (2015) A structural perspective on the regulation of the epidermal growth factor receptor. *Annu. Rev. Biochem.* **84,** 739–764 CrossRef Medline
11. Solit, D. B., and Rosen, N. (2007) Targeting HER2 in prostate cancer: where to next. *J. Clin. Oncol.* **25,** 241–243 CrossRef Medline
12. Traish, A. M., and Morgentaler, A. (2009) Epidermal growth factor receptor expression escapes androgen regulation in prostate cancer: a potential molecular switch for tumour growth. *Br. J. Cancer* **101,** 1949–1956 CrossRef Medline
13. Gross, M. E., Jo, S., and Agus, D. B. (2004) Update on HER-kinase-directed therapy in prostate cancer. *Clin. Adv. Hematol. Oncol.* **2,** 53–56, 64 Medline
14. Manole, S., Richards, E. J., and Meyer, A. S. (2016) JNK pathway activation modulates acquired resistance to EGFR/HER2 targeted therapies. *Cancer Res.* **76,** 5219–5228 CrossRef Medline
15. Feferman, L., Bhattacharyya, S., Deaton, R., Gann, P., Guzman, G., Kajdacsy-Balla, A., and Tobacman, J. K. (2013) Arylsulfatase B (*N*-acetylgalactosamine-4-sulfatase): potential role as a biomarker in prostate cancer. *Prostate Cancer Prostatic Dis.* **16,** 277–284 CrossRef Medline
16. Feferman, L., Deaton, R., Bhattacharyya, S., Xie, H., Gann, P. H., Melamed, J., and Tobacman, J. K. (2017) Arylsulfatase B is reduced in prostate cancer recurrences. *Cancer Biomark.* **21,** 229–234 CrossRef Medline
17. Bhattacharyya, S., Feferman, L., and Tobacman, J. K. (2014) Arylsulfatase B regulates versican expression by galectin-3 and AP-1 mediated transcriptional effects. *Oncogene* **33,** 5467–5476 CrossRef Medline
18. Bhattacharyya, S., Feferman, L., and Tobacman, J. K. (2014) Increased expression of colonic Wnt9A through Sp1-mediated transcriptional effects involving arylsulfatase B, chondroitin 4-sulfate, and galectin-3. *J. Biol. Chem.* **289,** 17564–17575 CrossRef Medline
19. Bhattacharyya, S., Feferman, L., Terai, K., Dudek, A. Z., and Tobacman, J. K. (2017) Decline in arylsulfatase B leads to increased invasiveness of melanoma cells. *Oncotarget* **8,** 4169–4180 Medline
20. Bhattacharyya, S., and Tobacman, J. K. (2012) Hypoxia reduces arylsulfatase B activity and silencing arylsulfatase B replicates and mediates the effects of hypoxia. *PLoS One* **7,** e33250 CrossRef Medline
21. Bhattacharyya, S., Feferman, L., and Tobacman, J. K. (2016) Inhibition of phosphatase activity follows decline in sulfatase activity and leads to transcriptional effects through sustained phosphorylation of transcription factor MITF. *PLoS One* **11,** e0153463 CrossRef Medline
22. Bhattacharyya, S., Feferman, L., and Tobacman, J. K. (2017) Chondroitin sulfatases differentially regulate Wnt signaling in prostate stem cells through effects on SHP2, phospho-ERK1/2, and Dickkopf Wnt signaling pathway inhibitor (DKK3). *Oncotarget* **8**, 100242–100260 Medline
23. Crawley, A., Ramsay, S. L., Byers, S., Hopwood, J., and Meikle, P. J. (2004) Monitoring dose response of enzyme replacement therapy in feline mu-

copolysaccharidosis type VI by tandem mass spectrometry. *Pediatr. Res.* **55,** 585–591 CrossRef Medline
24. Anson, D. S., Taylor, J. A., Bielicki, J., Harper, G. S., Peters, C., Gibson, G. J., and Hopwood, J. J. (1992) Correction of human mucopolysaccharidosis type-VI fibroblasts with recombinant *N*-acetylgalactosamine-4-sulphatase. *Biochem. J.* **284,** 789–794 CrossRef Medline
25. Rivera-Colón, Y., Schutsky, E. K., Kita, A. Z., and Garman, S. C. (2012) The structure of human GALNS reveals the molecular basis for mucopolysaccharidosis IVA. *J. Mol. Biol.* **423,** 736–751 CrossRef Medline
26. de Sousa, J. F., Jr., Nader, H. B., and Dietrich, C. P. (1990) Sequential degradation of chondroitin sulfate in molluscs. *J. Biol. Chem.* **265,** 20150–20155 Medline
27. Glaser, J. H., and Conrad, H. E. (1979) Chondroitin SO4 catabolism in chick embryo chondrocytes. *J. Biol. Chem.* **254,** 2316–2325 Medline
28. Ingmar, B., and Wasteson, A. (1979) Sequential degradation of a chondroitin sulfate disaccharide by lysosomal enzymes from embryonic-chick epiphysial cartilage. *Biochem. J.* **179,** 7–13 CrossRef Medline
29. Kotlo, K., Bhattacharyya, S., Yang, B., Feferman, L., Tejaskumar, S., Linhardt, R., Danziger, R., and Tobacman, J. K. (2013) Impact of salt exposure on *N*-acetylgalactosamine-4-sulfatase (arylsulfatase B) activity, glycosaminoglycans, kininogen, and bradykinin. *Glycoconj. J.* **30,** 667–676 CrossRef Medline
30. Chen, Y. N., LaMarche, M. J., Chan, H. M., Fekkes, P., Garcia Fontanet, J., Acker, M. G., Antonakos, B., Chen, C. H., Chen, Z., Cooke, V. G., Dobson, J. R., Deng, Z., Fei, F., Firestone, B., Fodor, M., *et al.* (2016) Allosteric inhibition of SHP2 phosphatase inhibits cancers driven by receptor tyrosine kinases. *Nature* **535,** 148–152 CrossRef Medline
31. Bunda, S., Burrell, K., Heir, P., Zeng, L., Alamsahebpour, A., Kano, Y., Raught, B., Zhang, Z. Y., Zadeh, G., and Ohh, M. (2015) Inhibition of SHP2-mediated dephosphorylation of Ras suppresses oncogenesis. *Nat. Commun.* **6,** 8859 CrossRef Medline
32. Tartaglia, M., Niemeyer, C. M., Fragale, A., Song, X., Buechner, J., Jung, A., Hählen, K., Hasle, H., Licht, J. D., and Gelb, B. D. (2003) Somatic mutations in PTPN11 in juvenile myelomonocytic leukemia, myelodysplastic syndromes and acute myeloid leukemia. *Nat. Genet.* **34,** 148–150 CrossRef Medline
33. Grossmann, K. S., Rosário, M., Birchmeier, C., and Birchmeier, W. (2010) The tyrosine phosphatase Shp2 in development and cancer. *Adv. Cancer Res.* **106,** 53–89 CrossRef Medline
34. Chan, G., Kalaitzidis, D., and Neel, B. G. (2008) The tyrosine phosphatase Shp2 (PTPN11) in cancer. *Cancer Metastasis Rev.* **27,** 179–192 CrossRef Medline
35. Wang, Q., Yang, Z. L., Zou, Q., Yuan, Y., Li, J., Liang, L., Zeng, G., and Chen, S. (2016) Shp2 and UGP2 are biomarkers for progression and poor prognosis of gallbladder cancer. *Cancer Invest.* **34,** 255–264 CrossRef Medline
36. LaRochelle, J. R., Fodor, M., Xu, X., Durzynska, I., Fan, L., Stams, T., Chan, H. M., LaMarche, M. J., Chopra, R., Wang, P., Fortin, P. D., Acker, M. G., and Blacklow, S. C. (2016) Structural and functional consequences of three cancer-associated mutations of the oncogenic phosphatase SHP2. *Biochemistry* **55,** 2269–2277 CrossRef Medline
37. Bard-Chapeau, E. A., Li, S., Ding, J., Zhang, S. S., Zhu, H. H., Princen, F., Fang, D. D., Han, T., Bailly-Maitre, B., Poli, V., Varki, N. M., Wang, H., and Feng, G. S. (2011) Ptpn11/Shp2 acts as a tumor suppressor in hepatocellular carcinogenesis. *Cancer Cell* **19,** 629–639 CrossRef Medline
38. Jiang, C., Hu, F., Tai, Y., Du, J., Mao, B., Yuan, Z., Wang, Y., and Wei, L. (2012) The tumor suppressor role of Src homology phosphotyrosine phosphatase 2 in hepatocellular carcinoma. *J. Cancer Res. Clin. Oncol.* **138,** 637–646 CrossRef Medline
39. Luo, X., Liao, R., Hanley, K. L., Zhu, H. H., Malo, K. N., Hernandez, C., Wei, X., Varki, N. M., Alderson, N., Chu, C., Li, S., Fan, J., Loomba, R., Qiu, S. J., and Feng, G. S. (2016) Dual Shp2 and Pten deficiencies promote non-alcoholic steatohepatitis and genesis of liver tumor-initiating cells. *Cell Rep.* **17,** 2979–2993 CrossRef Medline
40. Qi, C., Han, T., Tang, H., Huang, K., Min, J., Li, J., Ding, X., and Xu, Z. (2017) Shp2 inhibits proliferation of esophageal squamous cell cancer via dephosphorylation of Stat3. *Int. J. Mol. Sci.* **18,** E134 Medline
41. Hellmuth, K., Grosskopf, S., Lum, C. T., Würtele, M., Röder, N., von Kries, J. P., Rosario, M., Rademann, J., and Birchmeier, W. (2008) Specific inhibitors of the protein tyrosine phosphatase Shp2 identified by high-throughput docking. *Proc. Natl. Acad. Sci. U.S.A.* **105,** 7275–7280 CrossRef Medline
42. Rogerson, S. J., and Brown, G. V. (1997) Chondroitin sulfate A as an adherence receptor for *Plasmodium falciparum*-infected erythrocytes. *Parasitol. Today* **13,** 70–75 CrossRef Medline
43. Suhovskih, A. V., Mostovich, L. A., Kunin, I. S., Boboev, M. M., Nepomnyashchikh, G. I., Aidagulova, S. V., and Grigorieva, E. V. (2013) Proteoglycan expression in normal human prostate tissue and prostate cancer. *ISRN Oncol.* **2013,** 680136 CrossRef Medline
44. Edwards, I. J. (2012) Proteoglycans in prostate cancer. *Nat. Rev. Urol.* **9,** 196–206 CrossRef Medline
45. Sharpe, B., Alghezi, D. A., Cattermole, C., Beresford, M., Bowen, R., Mitchard, J., and Chalmers, A. D. (2017) A subset of high Gleason grade prostate carcinomas contain a large burden of prostate cancer syndecan-1 positive stromal cells. *Prostate.* **77,** 1312–1324 CrossRef Medline
46. Grindel, B., Li, Q., Arnold, R., Petros, J., Zayzafoon, M., Muldoon, M., Stave, J., Chung, L. W., and Farach-Carson, M. C. (2016) Perlecan/HSPG2 and matrilysin/MMP-7 as indices of tissue. invasion: tissue localization and circulating perlecan fragments in a cohort of 288 radical prostatectomy patients. *Oncotarget* **7,** 10433–10447 Medline
47. Reyes, N., Benedetti, I., Bettin, A., Rebollo, J., and Geliebter, J. (2016) The small leucine rich proteoglycan fibromodulin is overexpressed in human prostate epithelial cancer cell lines in culture and human prostate cancer tissue. *Cancer Biomark.* **16,** 191–202 CrossRef Medline
48. Xu, W., Neill, T., Yang, Y., Hu, Z., Cleveland, E., Wu, Y., Hutten, R., Xiao, X., Stock, S. R., Shevrin, D., Kaul, K., Brendler, C., Iozzo, R. V., and Seth, P. (2015) The systemic delivery of an oncolytic adenovirus expressing decorin inhibits bone metastasis in a mouse model of human prostate cancer. *Gene Ther.* **22,** 247–256 CrossRef Medline
49. Paulus, W., Baur, I., Dours-Zimmermann, M. T., and Zimmermann, D. R. (1996) Differential expression of versican isoforms in brain tumors. *J. Neuropathol. Exp. Neurol.* **55,** 528–533 CrossRef Medline
50. Serra, M., Miquel, L., Domenzain, C., Docampo, M. J., Fabra, A., Wight, T. N., and Bassols, A. (2005) V3 versican isoform expression alters the phenotype of melanoma cells and their tumorigenic potential. *Int. J. Cancer* **114,** 879–886 CrossRef Medline
51. Hernández, D., Miquel-Serra, L., Docampo, M. J., Marco-Ramell, A., Cabrera, J., Fabra, A., and Bassols, A. (2011) V3 versican isoform alters the behavior of human melanoma cells by interfering with CD44/ErbB-dependent signaling. *J. Biol. Chem.* **286,** 1475–1485 CrossRef Medline
52. Foulcer, S. J., Day, A. J., and Apte, S. S. (2015) Isolation and purification of versican and analysis of versican proteolysis. *Methods Mol. Biol.* **1229,** 587–604 CrossRef Medline
53. Wight, T. N. (2018) A role for proteoglycans in vascular disease. *Matrix Biol.* CrossRef Medline
54. Bhattacharyya, S., Kotlo, K., Shukla, S., Danziger, R. S., and Tobacman, J. K. (2008) Distinct effects of *N*-acetylgalactosamine-4-sulfatase and galactose-6-sulfatase expression on chondroitin sulfate. *J. Biol. Chem.* **283,** 9523–9530 CrossRef Medline
55. Zhang, X., Bhattacharyya, S., Kusumo, H., Goodlett, C. R., Tobacman, J. K., and Guizzetti, M. (2014) Arylsulfatase B modulates neurite outgrowth via astrocyte chondroitin-4-sulfate: dysregulation by ethanol. *Glia* **62,** 259–271 CrossRef Medline
56. Kim, S. O., Jiang, J., Yi, W., Feng, G. S., and Frank, S. J. (1998) Involvement of the Src homology 2-containing tyrosine phosphatase SHP-2 in growth hormone signaling. *J. Biol. Chem.* **273,** 2344–2354 CrossRef Medline
57. Liu, Z., Masuko, S., Solakyildirim, K., Pu, D., Linhardt, R. J., and Zhang, F. (2010) Glycosaminoglycans of the porcine central nervous system. *Biochemistry* **49,** 9839–9847 CrossRef Medline
58. Shen, Y., Tenney, A. P., Busch, S. A., Horn, K. P., Cuascut, F. X., Liu, K., He, Z., Silver, J., and Flanagan, J. G. (2009) PTPσ is a receptor for chondroitin sulfate proteoglycan, an inhibitor of neural regeneration. *Science* **326,** 592–596 CrossRef Medline

59. Holzberg, D., Knight, C. G., Dittrich-Breiholz, O., Schneider, H., Dörrie, A., Hoffmann, E., Resch, K., and Kracht, M. (2003) Disruption of the c-JUN-JNK complex by a cell-permeable peptide containing the c-JUN δ domain induces apoptosis and affects a distinct set of interleukin-1-induced inflammatory genes. *J. Biol. Chem.* **278,** 40213–40223 CrossRef Medline
60. Barr, R. K., Kendrick, T. S., and Bogoyevitch, M. A. (2002) Identification of the critical features of a small peptide inhibitor of JNK activity. *J. Biol. Chem.* **277,** 10987–10997 CrossRef Medline
61. Fanjul, A., Dawson, M. I., Hobbs, P. D., Jong, L., Cameron, J. F., Harlev, E., Graupner, G., Lu, X. P., and Pfahl, M. (1994) A new class of retinoids with selective inhibition of AP-1 inhibits proliferation. *Nature* **372,** 107–111 CrossRef Medline
62. Blume, S. W., Snyder, R. C., Ray, R., Thomas, S., Koller, C. A., and Miller, D. M. (1991) Mithramycin inhibits SP1 binding and selectively inhibits transcriptional activity of the dihydrofolate reductase gene *in vitro* and *in vivo*. *J. Clin. Invest.* **88,** 1613–1621 CrossRef Medline